ISSN 1070-3284, Russian Journal of Coordination Chemistry, 2015, Vol. 41, No. 6, pp. 387–394. © Pleiades Publishing, Ltd., 2015.
Original Russian Text © E.A. Katlenok, A.A. Zolotarev, A.Yu. Ivanov, S.N. Smirnov, R.I. Baichurin, K.P. Balashev, 2015, published in Koordinatsionnaya Khimiya, 2015, Vol. 41, No. 6, pp. 357–364.

Binuclear Platinated 2-Phenylbenzothiazole Complexes with Bridging 2-Mercapto Derivatives of Thiazoline, 1-Methylimidazole, and Pyrimidine: Structures and Optical and Electrochemical Properties

E. A. Katlenok[a], A. A. Zolotarev[b], A. Yu. Ivanov[b], S. N. Smirnov[b], R. I. Baichurin[a], and K. P. Balashev[a, *]

[a] *Russian State Pedagogical University, St. Petersburg, Russia*

[b] *St. Petersburg State University, St. Petersburg, Russia*

**e-mail: k_balashev@mail.ru*

Received November 4, 2014

Abstract—The structures of complexes $[Pt(Bt)(\mu\text{-}(N\hat{}S))]_2$ with platinated 2-phenylbenzothiazole (Bt) and bridging 2-mercapto derivatives (N^S) of thiazoline, 1-methylimidazole, and pyrimidine in the crystalline state and in a $CDCl_3$ solution are studied by X-ray diffraction analysis and ^1H, ^{13}C, and ^{195}Pt NMR spectroscopy. Complexes $[Pt(Bt)(\mu\text{-}(N\hat{}S))]_2$ have the *cis*-N(Bt),S(N^S) structure with the Pt–Pt chemical bond (2.89–2.93 Å) and antisymmetrical position of two cycloplatinated and two bridging ligands (CCDC nos. 1001204 (**I**), 1027021 (**II**), and 993566 (**III**)). The long-wavelength absorption bands (410–540 nm), phosphorescence bands with $\lambda_{max} = 685$ nm, and two-electron electroreduction ($E_p = -(2.00–2.27)$ V) and oxidation ($E_p = 0.07–0.20$ V) processes are assigned to photo- and electrostimulated processes involving the LUMO and HOMO predominantly localized on the π^* orbitals of {Pt(Bt)} and on the σ^* orbitals of the metal–metal chemical bond.

DOI: 10.1134/S1070328415060032

INTRODUCTION

The phosphorescence of the Pt(II) cyclometallated complexes with heterocyclic ligands in the solid state and in solutions at room temperature makes it possible to use them as triplet activators of organic photodiodes, photocatalysts, optical chemosensors, and luminescent labels of biosystems [1–5]. A change in the nature of the metallated and chelating ligands provides a possibility of modifying the optical and electrochemical characteristics of the complexes [6].

The planar structure of the cyclometallated Pt(II) complexes allows their association due to the d_z^2–d_z^2 and π–π interactions of the orbitals of the metal and ligand, which can lead to the formation of the Pt–Pt chemical bond and a change in the nature and energy of the highest occupied (HOMO) and lowest unoccupied (LUMO) molecular orbitals of the complexes, which is accompanied by the shift of the phosphorescence spectrum and oxidation and reduction potentials of Pt(II) [7–11]. The modification of the optical and electrochemical properties of the binuclear cyclometallated Pt(II) complexes with different distances between the platinum centers determined by the nature of the metallated and bridging ligands was shown [8, 10, 12]. Therefore, the extension of a range of ligands is urgent for the determination of the possibility for predicting the optical and electrochemical properties of these complexes.

In this work, we present the results of X-ray diffraction analysis, ^1H, ^{13}C, and ^{195}Pt NMR spectroscopy, absorption and emission electron spectroscopy, and voltammetry of the binuclear $[Pt(Bt)\mu\text{-}(N\hat{}S)]_2$ complexes with the cycloplatinated ligands: 2-phenylbenzothiazolate {Pt(Bt)} and bridging $(N\hat{}S)^-$ 2-mercapto derivatives of five-membered thiazoline $[Pt(Bt)(\mu\text{-Mtz})]_2$ (**I**), 1 and 1-methylimidazole $[Pt(Bt)(\mu\text{-Mim})]_2$ (**II**) and six-membered pyrimidine $[(Pt(Bt)(\mu\text{-Mpm})]_2$ (**III**).

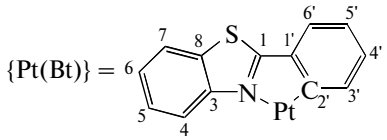

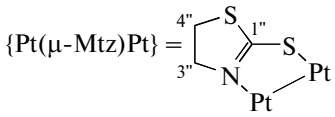

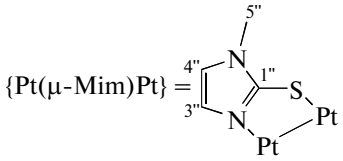

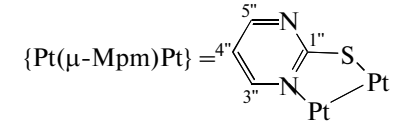

EXPERIMENTAL

The syntheses of complexes **I**, **II**, and **III** in ~50% yield and the preparation of their single crystals were conducted similarly to a described procedure [8] using the corresponding reagents (reagent grade). Analyses to the C, H, N, and S content in the complexes were carried out on an Evrovector EA3000 analyzer at the Center for Collective Use of the Chemical Department of the Russian State Pedagogical University (St. Petersburg).

For $C_{32}H_{24}N_4S_6Pt_2$ (**I**)

anal. calcd., %:	C, 36.71;	H, 2.31;	N, 5.35;	S, 18.37.
Found, %:	C, 37.02;	H, 2.47;	N, 5.24;	S, 18.41.

For $C_{34}H_{26}N_6S_4Pt_2$ (**II**)

anal. calcd., %:	C, 39.34;	H, 2.52;	N, 8.10;	S, 12.36.
Found, %:	C, 39.22;	H, 2.46;	N, 8.04;	S, 12.08.

For $C_{32}H_{22}N_6S_4Pt_2$ (**III**)

anal. calcd., %:	C 35.62;	H 2.06;	N 7.79;	S 11.89.
Found, %:	C 35.77;	H 2.17;	N 7.64;	S 12.03.

The ^1H and ^{13}C NMR spectra and the dqf-COSY, NOESY, $^1H-^{13}C$ HMQC, and $^1H-^{13}C$ HMBC spectra of complexes **I**, **II**, and **III** in solutions of $CDCl_3$ were recorded on a JNM-ECX400A spectrometer with working frequencies of 399.78 (^1H) and 100.53 MHz (^{13}C) at the Center for Collective Use of the Chemical Department of the Russian State Pedagogical University (St. Petersburg). Signals of the residual protons of the non-deuterated solvent served as an internal standard. ^{195}Pt NMR spectra in solutions of CD_2Cl_2 (86.015 MHz, 299 K) were recorded on a Bruker Avance III 400 spectrometer of the Resource Center "Magnetoresonance Investigation Methods" of the Scientific Park of the St. Petersburg State University.

^1H NMR (δ, ppm): bis((μ-2-mercaptothiazolinato)(2-phenyl-3-ido)benzothiazoleplatinum)(Pt–Pt) (**I**), 7.63 d ($2H^7$), 7.61 d ($2H^4$), 7.50 ddd ($2H^5$), 7.35 ddd ($2H^6$), 7.26 m ($2H^{3'}$), 7.05 dd ($2H^{6'}$), 6.62 ddd ($2H^{5'}$), 6.14 ddd ($2H^{4'}$), 4.57 dt ($2H^{3''a}$), 4.48 ddd ($2H^{3''b}$), 3.64 m ($2H^{4''a}$), 3.57 m ($2H^{4''b}$); bis((μ-2-mercapto-1-methylimidazolato)(2-phenyl-3-ido)benzothiazoleplatinum)(Pt–Pt) (**II**), 7.67 d ($2H^7$), 7.32 ddd ($2H^6$), 7.24 d ($2H^{3'}$), 7.22 ddd ($2H^5$), 7.11 d ($2H^{3''}$), 7.07 dd ($2H^{6'}$), 6.80 m ($4H^{4'',5'}$), 6.71 d ($2H^4$), 6.32 ddd ($2H^{4'}$), 3.57 s ($6H^{5''}$); bis((μ-2-mercaptopyridinato)(2-phenyl-3-ido)benzothiazoleplatinum)(Pt–Pt) (**III**), 8.97 d ($2H^{3''}$), 8.37 dd ($2H^{5''}$), 7.72 d ($2H^7$), 7.32 d ($2H^6$), 7.26 m ($4H^{5,3'}$), 7.08 d ($2H^{6'}$), 6.88 dd ($2H^{4''}$), 6.80 dd ($2H^{5'}$), 6.45 d ($2H^4$), 6.30 dd ($2H^{4'}$). ^{13}C NMR (δ, ppm): ($2C^1$), 176.6 ($2C^{1''}$), 150.5 ($2C^3$), 141.1 ($2C^{2'}$), 140.0 ($2C^{1'}$), 134.0 ($2C^{3'}$), 131.2 ($2C^8$), 128.3 ($2C^{4'}$), 127.3 ($2C^5$), 124.7 ($2C^6$), 124.3 ($2C^{6'}$), 122.8 ($2C^{5'}$), 122.0 ($2C^7$), 120.2 ($2C^4$), 64.5 ($2C^{3''}$), 34.7 ($2C^{4''}$); II – 181.6 ($2C^1$), 153.0 ($2C^{1''}$), 142.8 ($2C^{2'}$), 140.7 ($2C^{1'}$), 133.7 ($2C^{3'}$), 131.6 ($2C^8$), 129.1 ($2C^{4'}$), 128.1 ($2C^{3''}$), 126.5 ($2C^5$), 124.3 ($4C^{6,6'}$), 122.5 ($2C^{5'}$), 121.5 ($2C^7$), 120.2 ($2C^{4''}$) 120.7 ($2C^4$), 34.6 ($2C^{5''}$) NMR ^{195}Pt (δ, ppm): –3579.6 (**I**), –3595.7 (**II**).

Electronic absorption and emission spectra were recorded at 293 K on an SF-2000 spectrophotometer and a Flyuorat-02-Panorama spectrofluorimeter. Voltammograms were obtained on an IPC-PRO system in a cell with divided spaces of the working (glassy carbon, GS), auxiliary (Pt), and reference (Ag) electrodes in the presence of 0.1 M $[N(C_4H_9)_4]PF_6$ in a $C_6H_5CH_3$–CH_3CN (1 : 1) mixture. Peak potentials were presented with respect to a ferrocenium–ferrocene system at a rate of 100 mV/s.

The X-ray diffraction analyses of complexes **I–III** were carried out at 100 K on an Agilent Technologies Excaliburs Eos single-crystal diffractometer equipped with a planar detector of reflected X-rays of the CCD type (MoK_α radiation, λ = 0.71073 Å). The studies were carried out at the Resource Center "X-ray Diffraction Methods of Investigation" of the St. Petersburg State University. The crystallographic data and refinement parameters for structures **I–III** are given in Table 1. The relatively high refinement parameters for structure **II** are related to a low quality of the crystal. Strongly disordered solvent molecules were taken into account using the SQUEEZE function of the

Table 1. Crystallographic and refinement parameters for the structures of complexes **I**–**III**

Parameter	Value		
	I	**II**	**III**
FW	1047.14	1038.04	1079.01
Crystal system	Triclinic	Orthorhombic	Monoclinic
Space group	*P*1	*Pbca*	*C*2/*c*
Unit cell parameters:			
a, Å	12.1015(3)	11.1432(4)	7.2653(4)
b, Å	15.3938(4)	17.0872(4)	19.2162(10)
c, Å	18.5626(5)	35.4416(13)	21.0836(11)
α, deg	93.310(2)	90.00	90.00
β, deg	105.018(2)	90.00	92.755(5)
γ, deg	109.914(2)	90.00	90.00
V, Å^{3-}; *Z*	3099.32; 4	6748.3; 8	3001; 8
ρ(calcd), g/cm^3	2.244	2.043	2.286
μ, mm^{-1}	9.454	8.566	9.626
F(000)	1984.0	3944.0	1952.0
Range 2θ, deg	5.02–55.00	5.56–52.00	5.68–55.00
Index range	$-15 \le h \le 15$, $-19 \le k \le 19$, $-24 \le l \le 24$	$-13 \le h \le 12$, $-8 \le k \le 21$, $-43 \le l \le 42$	$-9 \le h \le 9$, $-24 \le k \le 24$, $-27 \le l \le 27$
Total number of reflections	56961	25965	10018
Number of independent reflections (R_{int})	14061 (0.0743)	6615 (0.0649)	3391 (0.0369)
Goodness-of-fit	1.057	1.074	1.083
R-factors ($F_0 \ge 4\sigma F$)	$R_1 = 0.046$ $wR_2 = 0.0705$	$R_1 = 0.069$ $wR_2 = 0.1392$	$R_1 = 0.029$ $wR_2 = 0.0530$
R-factors (all data)	$R_1 = 0.077$ $wR_2 = 0.0789$	$R_1 = 0.083$ $wR_2 = 0.1471$	$R_1 = 0.038$ $wR_2 = 0.0564$
$\Delta\rho_{min}/\Delta\rho_{max}$, *e* Å^{-3}	1.73/–1.72	5.32/–2.61	1.25/–1.53

$R_1 = \Sigma\|F_o| - |F_c\|/\Sigma|F_o|$; $wR_2 = \{\Sigma[w(F_o^2 - F_c^2)^2]/\Sigma[w(F_o^2)^2]\}^{1/2}$; $w = 1/[\sigma^2(F_o^2) + (aP)^2 + bP]$, where $P = (F_o^2 + 2F_c^2)/3$; $s = \{\Sigma[w(F_o^2 - F_c^2)]/(n-p)\}^{1/2}$, *n* is the number of reflections, *p* is the number of refined parameters.

PLATON program package [13]. The unit cell parameters for structures **I**–**III** were refined by least squares. The structures were solved by direct methods and refined using the SHELXL program [14] in the OLEX2 program package [15]. An absorption correction was applied empirically in the CrysAlisPro program package [16] using spherical harmonics accomplished in the SCALE3 ABSPACK scaling algorithm. Hydrogen atoms were included into the refinement with the fixed positional and temperature parameters calculated using the algorithms inserted in the SHELX program package. The CIF files containing an information on the structures of the complexes were deposited with the Cambridge Crystallographic Data Centre (CCDC 1001204 (**I**), 1027021 (**II**), and 993566 (**III**); site www.ccdc.cam.ac.uk/data_request/cif).

RESULTS AND DISCUSSION

A unit cell of single crystals of complexes **I**–**III** contains *cis*-N(Bt),S(N^S) isomers of [Pt(Bt)(μ-(N^S))]$_2$ with the Pt–Pt chemical bond (2.89–2.93 Å) and the antisymmetrical spatial position of two cycloplatinated and two bridging ligands (Fig. 1). Unlike complexes **II** and **III**, the intermolecular hydrogen bonds (S···H 3.15–3.50 Å) between the S atoms and

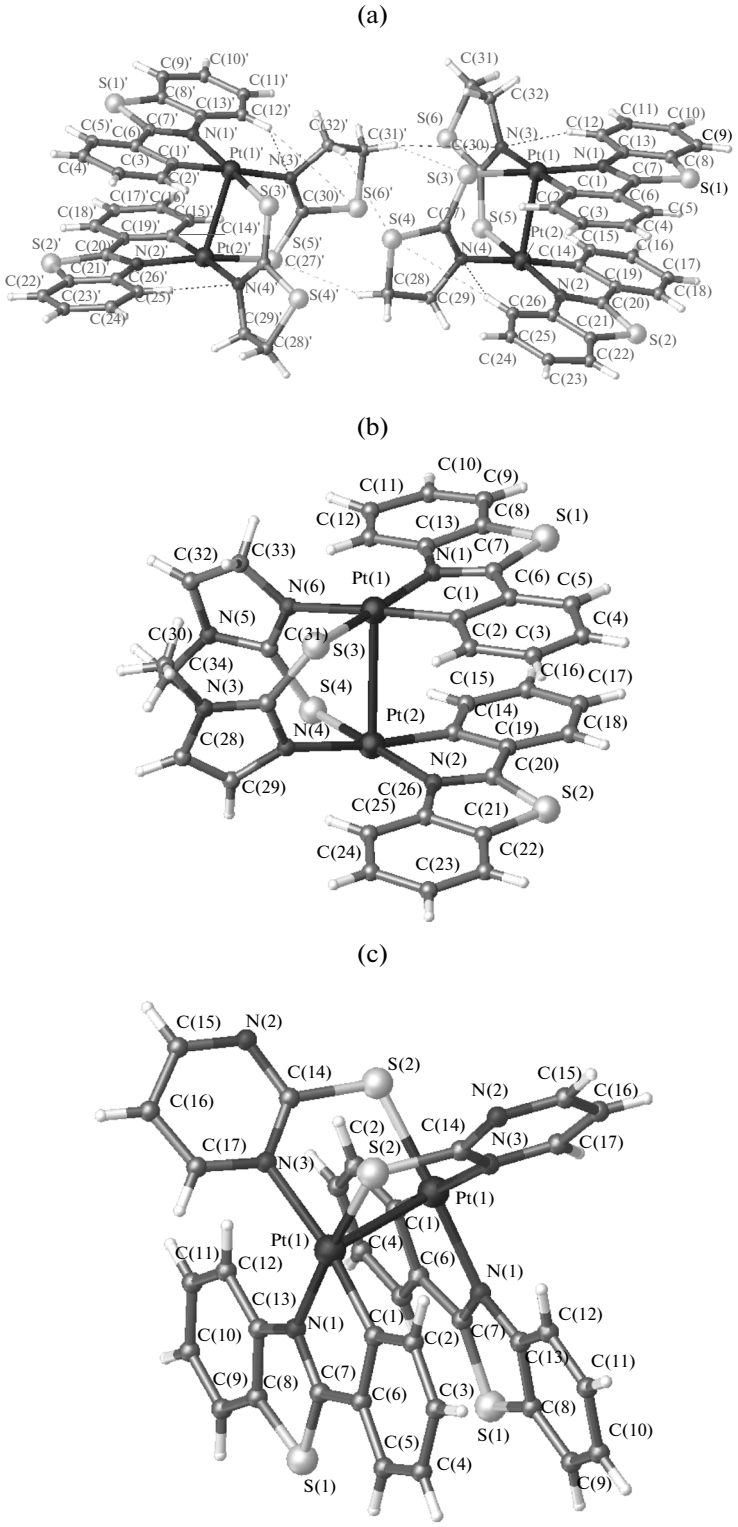

Fig. 1. Molecular structures of complexes (a) **I**, (b) **II**, and (c) **III**.

H(4'') atoms of the bridging 2-mercaptopyrazoline ligands of the adjacent molecules of complex **I** predetermine the existence of a dimer (Fig. 1a) in the unit cell.

The bond lengths and bond angles of the donor atoms of the ligands with the platinum centers of the complexes (Table 2) change insignificantly ($\Delta d \leq$

Table 2. Bond lengths (Å) and bond angles (deg) for complexes **I**–**III**

Bond	**I**		**II**	**III**
	d, Å			
Pt–Pt	2.9202(4)	2.9327(4)	2.9917(7)	2.8888(3)
Pt–C(Bt)	2.003(7) 2.001(8)	2.003(8) 1.991(8)	2.02(1) 2.00(1)	1.993(4) 1.993(4)
Pt–N(Bt)	2.073(6) 2.072(6)	2.079(6) 2.071(6)	2.07(1) 2.06(1)	2.097(4) 2.097(4)
Pt–N(N^S)	2.133(6) 2.101(6)	2.137(6) 2.105(6)	2.12(1) 2.12(1)	2.135(4) 2.135(4)
Pt–S(N^S)	2.286(2) 2.275(2)	2.278(2) 2.276(2)	2.287(4) 2.286(4)	2.280(1) 2.280(1)
Angle	ω, deg			
N(Bt)PtC(Bt)	81.0(3) 80.6(3)	81.3(3) 80.3(3)	80.4(5) 80.3(4)	81.3(2) 81.3(2)
N(Bt)PtN(N^S)	99.1(2) 96.9(2)	98.4(3) 96.7(2)	100.2(4) 98.5(4)	98.6(1) 98.6(1)
N(N^S)PtS(N^S)	88.1(2) 86.7(2)	87.3(2) 86.4(2)	86.8(3) 86.9(3)	86.7(1) 86.7(1)
S(N^S)PtC(Bt)	93.9(2) 93.4(2)	94.9(2) 92.1(2)	94.5(4) 93.4(3)	93.3(1) 93.3(1)
S(N^S)C(N^S)N(N^S)	129.6(6) 128.4(6)	129.0(6) 129.0(6)	128(1) 125(1)	122.9(3) 122.9(3)

Table 3. Coordination-induced chemical shifts ($\delta_{complex} - \delta_{free\ ligand}$, ppm) of the ligand atoms in the ^1H and ^{13}C NMR spectra of the complexes in a $CDCl_3$ solution

Complex	^1H, ^{13}C	Atom no.										
		4	5	6	7	3'	4'	5'	6'	3"	4"	5"
		{Pt(Bt)}								{Pt(μ-(N^S)}		
I	^1H	−0.5	0.0	−0.1	−0.3	−0.2	−1.3	−0.9	−1.0	1.0	−0.4	
	^{13}C	−2.8	1.3	−0.3	0.6	5.6	−0.5	−5.6	−3.0	13.0	1.0	
II	^1H	−1.4	−0.3	−0.2	−0.3	−0.3	−1.1	−0.7	−1.0	0.4	0.0	0.0
	^{13}C	−2.3	0.5	−0.7	0.1	5.3	0.3	−5.9	−3.0	8.8	5.9	0.4
III	^1H	−1.5	−0.2	−0.2	−0.2	−0.2	−1.1	−0.7	−1.0	0.5	−0.1	−0.1

0.04 Å, $\Delta\omega \leq 3.5°$), depending on the nature of the bridging ligands. The sum of bond angles at the C, N, N, and S donor atoms of the ligands with the platinum centers ($\Sigma\omega = 346.1°$–$351.5°$) in complexes **I–III** corresponds to that of the planar coordination of the Pt atom. The decrease in the SCN bond angle of the S donor atom of the bridging ligand with the six-membered pyrimidine cycle by ~7° compared to those in the five-membered imidazole and thiazoline cycles is accompanied by the corresponding shortening of the Pt–Pt chemical bond in the binuclear complexes by ~0.06 Å.

Unlike the bridging ligands, the planes of the antisymmetrical platinated 2-phenylbenzothiazole ligands in the composition of the binuclear complexes are nearly planar (±2.1° Å). Along with the short (~2.9 Å) distance and the d_z^2–d_z^2 interaction of the platinum centers, this indicates a possibility of their π–π interaction leading to both the anisotropic action

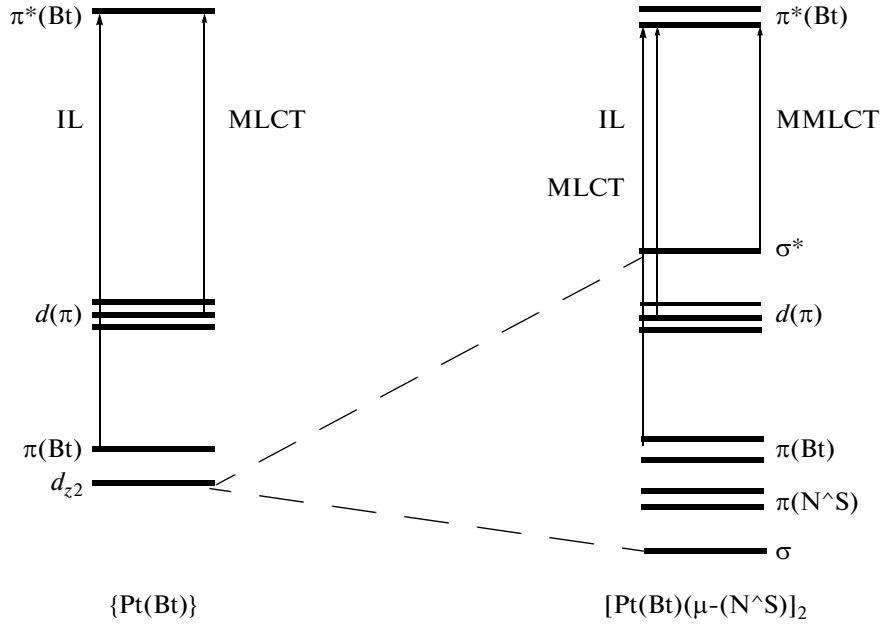

Fig. 2. Qualitative diagram of molecular orbitals for the $[Pt(Bt)(\mu\text{-}(N\hat{}S))]_2$ complexes.

of circular currents and the displacement of upfield chemical shifts of protons and a change in the energy of the π* orbitals of the platinated ligands.

The results of ^1H, ^{13}C, and ^{195}Pt NMR spectroscopy indicate similar molecular structures of binuclear complexes **I–III** in $CDCl_3$ solutions and in the crystalline state. This is indicated by a magnetic equivalence of the platinum centers and the H and C atoms of two metallated and two bridging ligands of the complexes and a significant upfield shift of the ^1H resonances of the metallated ligands in the NMR spectrum (Table 3).

In the framework of the model of predominantly localized molecular orbitals [17] and qualitative diagram of molecular orbitals (Fig. 2), the electronic absorption spectra of complexes **I–III** are characterized by three types of spin-allowed bands (Table 4). Intense ($\varepsilon > 10^4$ L mol^{-1} cm^{-1}) bands, whose position insignificantly differs from that of the free ligands, are observed at $\lambda < 330$ nm (Fig. 3). These bands were assigned to intraligand (IL) optical π–π* transitions. The absorbance with λ_{max} = 370–390 nm and ε = (5.9–12.0) × 10^3 L mol^{-1} cm^{-1} typical of the complexes with platinated 2-phenylbenzothiazole [9, 18, 19] was attributed to the metal-to-ligand charge-transfer (MLCT) transition d_π–π*(Bt). The longest-wavelength absorption bands at 425–540 nm with ε = (3.9–2.2) × 10^3 L mol^{-1} cm^{-1} were ascribed to metal–metal-to-ligand charge-transfer (MMLCT) optical transitions between the σ* HOMO formed by the Pt–Pt

Table 4. Optical and electrochemical parameters of complexes **I–III**

Complex	Absorption (λ, nm ($\varepsilon \times 10^3$ L mol^{-1} cm^{-1}))	Emission (λ, nm ($\Delta\nu_{1/2}$, cm^{-1}; τ, μs))	Excitation (λ, nm)	Reduction ($E_{1/2}$, V)	Oxidation (E_p, V)
I	261 (32.2), 314 (20.5), 332 sh (15), 374 sh (7.1), 392 sh (5.9), 431 sh (3.3), 477 sh (2.6), 492 (2.68), 535 sh (2.0)	685 (2500; 6)	389, 424, 442 sh, 462 sh, 488, 529	–2.23	0.16
II	261 (42.0), 295 (27.2), 313 (28.6), 334 sh (19), 384 (10.5), 411 sh (6.0), 478 sh (3.4), 540 sh (1.1)	685 (2700; 6)	388, 424, 443, 463 sh, 486, 531	–2.27	0.07
III	272(29.7), 308(31.3), 330 sh (22), 366(12.0), 426 sh (3.9), 478 sh (3.0), 495 (3.03), 504 sh (3.0), 530 sh (2.2)	685 (2600; 6)	382, 424, 442 sh, 462, 486, 529	–2.00	0.20

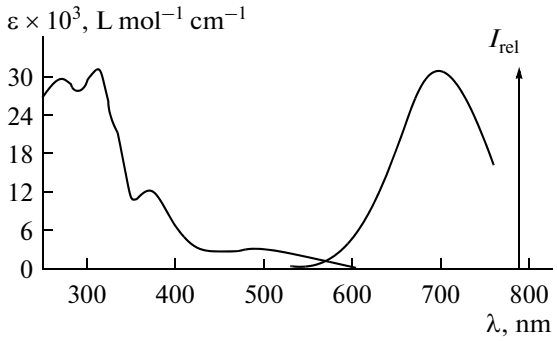

Fig. 3. Absorption and emission spectra of [Pt(Bt)(μ-Mpm)]$_2$ in a CH_2Cl_2 solution.

interaction and lower-energy π* orbitals of the heterocyclic ligands. The position of the long-wavelength absorption bands of the complexes is independent of the nature of the bridging ligands, indicating the predominant localization of the LUMO on the π* orbitals of the platinated 2-phenylbenzothiazole ligands.

The photoexcitation of solutions of the complexes in the range of long-wavelength absorption bands results in the appearance (Fig. 3) of characteristic [8, 9, 11, 17, 18] broad luminescence bands with a maximum at 685 nm, a half-width of 2500–2700 cm^{-1}, and an exponential decay time of 6–8 μs assigned to the MMLCT spin-forbidden optical transition. The phosphorescence excitation spectra are consistent with the absorption spectra of the complexes (Table 4), indicating that the radiation process proceeds from the lowest electron-excited state according to the Kasha rule [20].

The reduction voltammograms of complexes **I–III** are characterized by two-electron irreversible and quasi-reversible waves with the potentials of the current peaks –2.00…–2.27 V (Table 4) that insignificantly differ from the reduction potential of the mononuclear complex [Pt(Bt)En]$^+$ (En is ethylenediamine) at –2.17 V [21]. This makes it possible to assign these waves to ligand-centered processes of the electron transfer to the π* orbitals predominantly localized on the platinated 2-phenylbenzothiazole ligands acting as LUMO of the binuclear complexes

$$[Pt^{II}(Bt)(\mu\text{-}(N\hat{}S))]_2 + 2e^- = [Pt^{II}(Bt^-)(\mu\text{-}(N\hat{}S))]_2.$$

The cathodic shift of the potential of the ligand-centered electron transfer to the π* orbital predominantly localized on the platinated 2-phenylbenzothiazole ligands of the complexes in a series **I** ≈ **II** > **III** (Table 4) reflects, probably, a decrease in the efficiency of the π*–π* interaction of the platinated ligands with the elongation of the Pt–Pt chemical bond (Table 2).

The irreversible two-electron oxidation waves of the complexes with the potentials of the current peak 0.07–0.20 V (Table 4) were attributed to the metal-centered process involving the σ* HOMO

$$[Pt^{II}(Bt)(\mu\text{-}(N\hat{}S))]_2 - 2e^- = [Pt^{III}(Bt)(\mu\text{-}(N\hat{}S))]_2.$$

The cathodic shift of the potentials of the current peak of the irreversible oxidation waves of binuclear complexes **I–III** compared to the mononuclear complex [Pt(Bt)En]$^+$ (E_p = 1.05 V) [21] by ~0.9 V is consistent (Fig. 2) with the increased energy of the σ* HOMO of the binuclear complexes with the Pt–Pt chemical bond compared to the d_π HOMO of the mononuclear complexes.

The results of this work show the N(Bt),S(N^S) structure of the platinated 2-phenylbenzothiazole complexes [Pt(Bt)(μ-(N^S))]$_2$ with the bridging 2-mercapto derivatives of thiazoline, 1-methylimidazole, and pyrimidine in the crystalline state and in solutions. Similarly to earlier studied [Pt(C^N)(μ-Pyt)]$_2$ (μ-Pyt is bridging 2-mercaptopyridine) [8], the optical and electrochemical properties of the complexes are determined by the LUMO predominantly localized on the π* orbitals of platinated 2-phenylbenzothiazole and HOMO (σ* orbital of the metal–metal chemical bond). A change in the nature of the bridging ligand (μ-Mtz, μ-Mim, μ-Mpm) changes the energy of the LUMO and HOMO of the [Pt(Bt)(μ-S^N)]$_2$ complexes due to a change in the efficiency of the interaction of the d_z^2(Pt)–d_z^2(Pt) and π*(Bt)–π*(Bt) orbitals.

ACKNOWLEDGMENTS

This work was supported by the Ministry of Education and Science of the Russian Federation, state task no. 4.131.2014K.

REFERENCES

1. Williams, J.A.G., Develay, S., Rochester, D.L., et al., *Coord. Chem. Rev.*, 2008, vol. 252, nos 23–24, p. 2596.
2. You, Y. and Nam, W., *Chem. Soc. Rev.,* 2012, vol. 41, no. 21, p. 7061.
3. Goldsmith, G.I., Hudson, W.R., Lowry, M.S., et al., *J. Am. Chem. Soc.,* 2005, vol. 127, no. 20, p. 7502.
4. Rogers, C.W. and Wolf, M.O., *Coord. Chem. Rev.*, 2002, vols. 233–234, p. 341.
5. Yang, Y., Zhao, Q., Feng, W., et al., *Chem. Rev.*, 2013, vol. 113, no. 1, p. 192.
6. Zhao, J., Ji, S., Wu, W., et al., *RSC Adv.*, 2012, vol. 2, p. 1712.
7. Bercaw, J.E., Durell, A.C., Gray, H.B., et al., *Inorg. Chem.*, 2010, vol. 49, no. 4, p. 801.
8. Aoki, R., Kobayashi, A., Chang, H.-C., et al., *Bull. Chem. Soc. Jpn.*, 2011, vol. 84, no. 2, p. 18.
9. Katlenok, E.A. and Balashev, K.P., *Opt. Spectrosc.*, 2014, vol. 116, no. 1, p. 100.
10. Chakraborty, A., Deaton, J.C., Haefele, A., et al., *Organometallics*, 2013, vol. 32, no. 14, p. 3819.
11. Sicilia, V., Fornies, J., Casas, J.M., et al., *Inorg. Chem.*, 2012, vol. 51, no. 6, p. 3427.

12. Ma, B., Li, J., Djurovich, P.I., et al., *J. Am. Chem. Soc.*, 2005, vol. 127, no. 1, p. 28.

13. Spek, A.L., *Acta Crystallogr., Sect. D: Biol. Crystallorg.*, 2009, vol. 65, no. 2, p. 148.

14. Sheldrick, G.M., *Acta Crystallogr., Sect. A: Found. Crystallogr.*, 2008, vol. 64, no. 1, p. 112.

15. Dolomanov, O.V., Bourhis, L.J., Gildea, R.J., et al., *J. Appl. Crystallogr.,* 2009, vol. 42, no. 2, p. 339.

16. CrysAlisPro. Agilent Technologies. Version 1.171.36.20 (release 27-06-2012).

17. DeArmond, K., Hanck, K.W., and Wertz, D.W., *Coord. Chem. Rev.*, 1985, vol. 64, p. 65.

18. Katlenok, E.A. and Balashev, K.P., *Opt. Spectrosc.*, 2013, vol. 114, no. 5, p. 756.

19. Katlenok, E.A. and Balashev, K.P., *Opt. Spectrosc.*, 2014, vol. 117, no. 3, p. 374.

20. Kasha, M., *Discuss. Faraday Soc.*, 1950, vol. 9, no. 1, p. 14.

21. Katlenok, E.A., Zolotarev, A.A., and Balashev, K.P., *Russ. J. Coord. Chem.*, 2015, vol. 41, no. 1, p. 37.

Translated by E. Yablonskaya